

# Thermal and Rheological Behavior of Ultrafine Fly Ash Filled LDPE Composites

S. A. R. Hashmi, Pratibha Sharma, Navin Chand

Advanced Materials and Processes Research Institute (AMPRI), Council of Scientific and Industrial Research, Bhopal 462026, India

Received 4 September 2006; accepted 5 August 2007

DOI 10.1002/app.27351

Published online 5 November 2007 in Wiley InterScience (www.interscience.wiley.com).

**ABSTRACT:** The specimens containing different volume fractions of ultrafine fly ash in LDPE were prepared with the help of two roll mixing mill and the hot-plate compression-molding machine. Thermal and rheological properties were evaluated using DSC and parallel-plate rotational-rheometer. The effect of composition variation on melt enthalpy, crystallinity, shear viscosity, shear stress and first normal stress difference was studied and reported here. The addition of ultrafine fly ash in LDPE decreased the melt enthalpy of the specimen. Slight decrease in the crystallinity of LDPE was observed on addition of fly ash. The shear stress as well as the shear

viscosity both increased with the addition of ultrafine fly ash in LDPE. Two regions of shear thinning were observed at 200°C for fly ash filled LDPE. The first normal stress difference ( $N_1$ ) reduced with fly ash content and with the increased temperature. The values of  $N_1$  remained almost invariable at low shear region however a proportional increase was observed beyond the shear stress of 10 kPa. © 2007 Wiley Periodicals, Inc. *J Appl Polym Sci* 107: 2196–2202, 2008

**Key words:** ultrafine fly ash; LDPE; thermal properties; rheology

## INTRODUCTION

The functional fillers are used in polymer industry in large quantities to improve several desired properties. These fillers improve dimensional stability, reduce dielectric losses, enhance thermal and electrical insulation properties, and also modify the wear and friction characteristics of the composites.<sup>1–5</sup> In addition to several commercial fillers such as silica, calcium carbonate, talc, carbon black, rutile, etc., the fly ash has been incorporated in polymers to improve mechanical, thermal, and electrical properties. Fly ash has also been used in the development of functionally graded polymer composites to obtain gradient in density, hardness and electrical properties.<sup>6</sup> It has been advocated that fly ash can be used as filler or the supporting filler in the polymers.<sup>7</sup> The fine fly ash particles improve dielectric properties, rigidity and heat deflection temperature of polymers. Moreover the use of ultrafine particles (<10  $\mu\text{m}$ ), significantly affects the properties of composites due to the large specific surface of particles.<sup>8</sup>

The fly ash is a by-product obtained by combustion of coal in thermal power plants. It is driven away from the boiler by the gases and extracted out from them by mechanical collectors or electrostatic

precipitators or a combination of both. The disposal of fly ash poses serious environmental threat by contaminating the surrounding atmosphere and occupies huge land area for its dumping.<sup>9</sup> It is a mixture of oxides rich in silica ( $\text{SiO}_2$ ), iron ( $\text{Fe}_2\text{O}_3$ ), and aluminum ( $\text{Al}_2\text{O}_3$ ). The incorporating fly ash particles in polymers can improve the shortcomings associated with polymers such as high shrinkage, low stiffness, poor dimensional stability, and low flame resistance, etc. The chemical stability of the blends was also reported improved on adding fly ash in polypropylene/polycarbonate blend.<sup>10</sup> A few commercial polymer-based products contain fly ash; for example: floor tiles, sinks, automobile body, furniture, textile bobbins, flame-resistant electronic products etc.<sup>9,11</sup>

Many technical papers are available in the literature<sup>1–10</sup> related to the material characteristics in solid state but the behavior of fly ash filled polymers in molten state is rarely reported.<sup>6,10</sup> The properties of a composite in melt-form depend upon the shear history of melt. The macromolecules in particular, carry shear history and affect the microstructure as well. The behavior of particulate filled non-Newtonian polymer fluids such as molten polymers is very complicated. The combination of viscous and elastic components of the flow plays important role in a final design of composite material.

In this article we investigated the thermal and rheological properties of ultrafine fly ash filled low density-polyethylene (LDPE) composites. The effect of composition variation on melting enthalpy,

Correspondence to: Dr. S. A. R. Hashmi (sarhashmi@rediffmail.com).

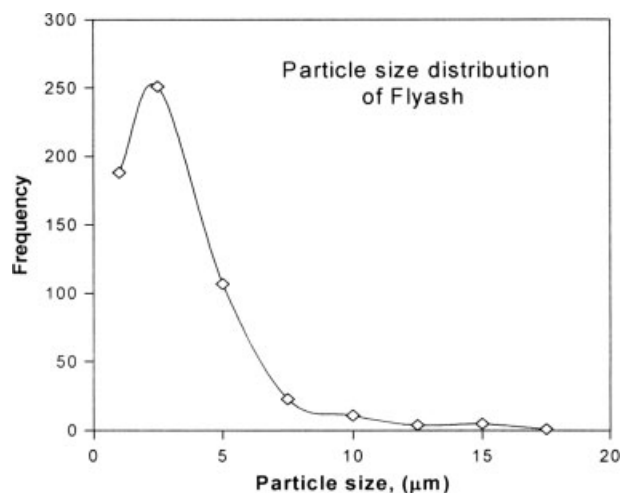


Figure 1 Size distribution curve of fly ash particles.

crystallinity, shear-stress, shear-viscosity, and first normal-stress difference was studied and reported here.

## MATERIALS AND METHODS

LDPE (grade 16MA 400) was obtained from Indian Petro-Chemicals (IPCL), India. Fly ash was obtained from NTPC Sarni, India. The major constituents of fly ash were:  $\text{Al}_2\text{O}_3$  30.94%,  $\text{SiO}_2$  57.64%,  $\text{Fe}_2\text{O}_3$  6.47%, the oxides of sodium, calcium and magnesium 3.47%, loss in ignition 0.52% by weight. The majority of particles were below 10  $\mu\text{m}$ . The particle size distribution curve is shown in Figure 1 and SEM of a representative sample of fly ash is given in Figure 2.

### Sample preparation

The various fractions of fly ash and LDPE as shown in Table I were mixed on Two Roll Mixing Mill at

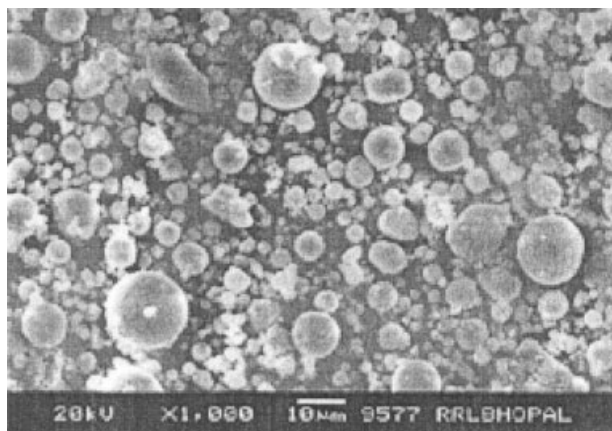


Figure 2 SEM photograph of fly ash particles.

TABLE I  
Composition of the Samples

S. no.	Sample designation	LDPE (g)	Fly ash (g)	Vol % of flyash (calculated)
1	LDPE	100	00	0.0
2	LD90FA10	90	10	4.24
3	LD80FA20	80	20	9.08
4	LD70FA30	70	30	14.63
5	LD60FA40	60	40	21.05
6	LD50FA50	50	50	28.56

140°C. The mixed material was removed from the mixer and was then cut to small pieces and was compression molded into 2-mm-thick sheets by using a hot-plate, hydraulic, compression-molding machine. The temperature of hot plates was 160°C and 5 MPa pressure was applied on molds. After 5 min the molds were cooled down to ambient temperature using circulation of water at 18°C. The samples were removed. The test specimens were cut from 2-mm-thick sheet for rheological studies. At least two specimens of 20 mm diameter were tested in each case for rheological tests.

### Rheological studies

Rheological properties were evaluated by using RS 600 rheometer of Thermo Electron Corp. The diameter of test specimen was 20 mm and tests were conducted using parallel plate having 20 mm diameter. The temperature of specimen was controlled by TC 501. The rheological tests were conducted at three different temperatures: 160, 180, and 200°C. The steady state shear rate was varied within the range of  $10^{-4}$  to  $10^2 \text{ s}^{-1}$  in steps. The first normal stress difference was also evaluated using normal force measurement on RS600 rheometer.

### SEM

Particles of fly ash were examined for their size distribution using scanning electron microscope model JSM 5600, JEOL, Japan. SEM micrographs were obtained from a representative sample of fly ash. The particle sizes of fly ash were determined by comparing length of distance bar appeared on micrograph. The particles were grouped in different particle size ranges and the frequency of particles was noted down. The size distribution was then presented in graphical form as shown in Figure 1. Fly ash particles as observed under scanning electron microscope are shown in Figure 2. The distribution of fly ash in LDPE matrix was also examined using SEM of fractured surfaces and is shown in Figure 3.

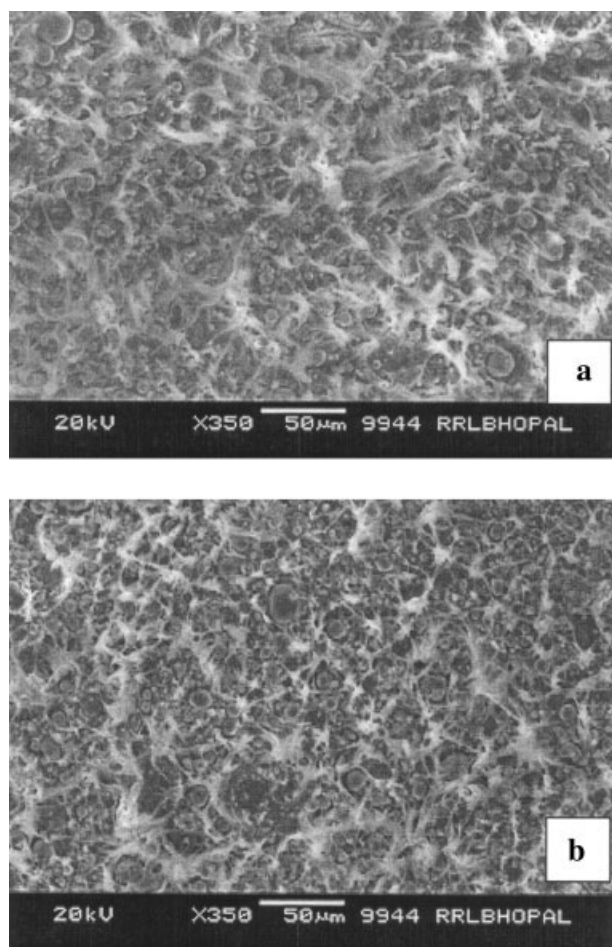


**Figure 3** SEM of fractured surfaces of (a) LD70FA30 and (b) LD50FA50.

### Differential scanning calorimetry

Differential scanning calorimetry (DSC) analysis was carried out using Mettler DSC 822/700/1447. The instrument was computer controlled and calculations were done using its software. It was calibrated using the onset temperature of melting of indium standards as well as the melting enthalpy of indium. Three to five milligrams of samples were sealed in aluminum pans and heated from 60°C to 200°C at a heating rate of 10°C min<sup>-1</sup>. Onset and peak temperatures of melting were determined.

## RESULTS AND DISCUSSION

The specific surface area of particulate fillers varies with the particle size and affects the mechanical as well as rheological properties of composites. Figure 1 shows plot between the frequency and the size of the studied fly ash particles. The population densities of finer particles are higher as compared to the larger particles. Mostly, the particle size was below 7 μm. A small fraction of particles lies in between 10

and 18 μm. Though the distribution curve provides information about particle size but the SEM photograph as shown in Figure 2 gives a better idea about the presence of larger particles, though less in number but occupy a significant volume, nearly 10 vol % of total particles. The nonuniform distribution of particles often gives different results particularly when sample size of composite is small and therefore care has been taken to test two or more samples for rheology to improve reliability of data in these experiments. To observe distribution of fly ash particles in LDPE matrix, the fractured surfaces were observed by SEM. Figure 3(a,b) shows SEM of impact-fractured surfaces of samples a) LD70FA30 and b) LD50FA50 respectively. Both LDPE and the fly ash particles can be seen in the micrographs. The fly ash particles were mostly in spherical shape and distributed uniformly in the composites as shown in Figure 3. LDPE on the other hand was observed with characteristic ductile failure mode.

Figure 4 shows enthalpy versus temperature curves for unfilled and fly ash filled LDPE of different compositions. The endothermic melt peaks of all the studied compositions are shown in this figure. The enthalpy data is given in Table II. It was observed that addition of fly ash causes little change in the melting point. Nature of curves does not vary significantly. While comparing with the different compositions, the enthalpies of test samples reduced with the increased fly ash content in the LDPE.

The values of enthalpy obtained from DSC curves were normalized for unit weight. The differences were observed in the normalized enthalpy and the expected enthalpy of fly ash filled LDPE as shown in Table II. The normalized enthalpy was determined based on the unit weight of samples whereas expected enthalpy was calculated based on the weight-fractions of LDPE and the fly ash in the samples, assuming that LDPE melting mechanism does

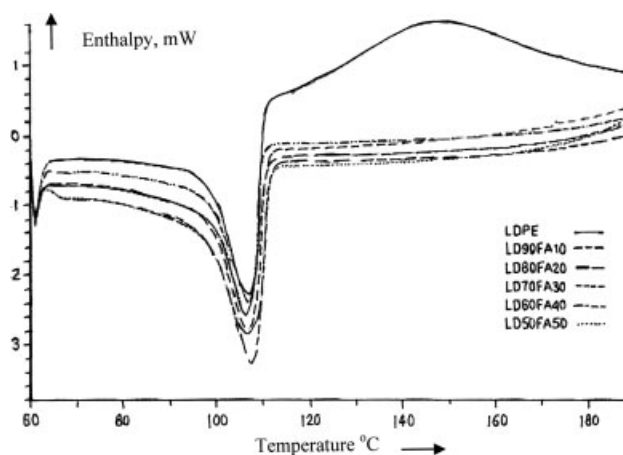


**Figure 4** DSC curves of LDPE and fly ash filled LDPE.

TABLE II  
DSC Analysis of Unfilled and Fly Ash Filled LDPE Composites

S. no.	Sample name	$T_o$ (°C)	$T_p$ (°C)	$T_l$ (°C)	$\Delta H_N$ (J g <sup>-1</sup> )	$\Delta H_E$ (J g <sup>-1</sup> )	$\alpha$ (%)
1	LDPE	97.93	106.58	110.14	-54.04	-54.01	18.44
2	LD90FA10	97.51	106.51	110.50	-44.54	-49.64	16.89
3	LD80FA20	97.56	105.85	110.51	-41.72	-45.25	17.79
4	LD70FA30	97.42	106.56	110.89	-35.54	-40.72	17.32
5	LD60FA40	98.44	106.07	110.39	-30.79	-36.16	17.51
6	LD50FA50	97.70	106.75	109.57	-25.20	-31.64	17.31

$T_o$ , onset temperature of melting;  $T_p$ , peak temperature of melting;  $T_l$ , temperature reaching liquid state;  $\Delta H_N$ , normalized enthalpy;  $\Delta H_E$ , estimated enthalpy;  $\alpha$ , crystallinity of LDPE in the sample.

not change in the presence of fly ash particles. It was expected that fly ash particles will be situated in the amorphous part of LDPE and may not affect the crystallization of LDPE but the estimated enthalpy of the fly ash filled LDPE was found higher as compared to the observed one in each case. It indicates that the addition of fly ash in LDPE has negative effect on crystallinity of LDPE. The fly ash particles might locate themselves in the interlamellar space, which restricts the crystallization process and might result in reduced enthalpy, as was found in case of copper filled LDPE.<sup>12</sup> The SEM micrographs also show that ultrafine fly ash particles have been distributed within the LDPE matrix and those might locate themselves in the interlamellar space.

Table II shows the crystalline percentage of LDPE in unfilled as well as fly ash filled composites, which was calculated using the standard value of enthalpy as 293 J g<sup>-1</sup> for the 100% crystalline LDPE from the literature.<sup>13</sup> It was ensured before the DSC test that all the samples including unfilled LDPE were subjected to same process conditions. The crystallinity ( $\alpha$ ) was evaluated by the following equation,<sup>13</sup>

$$\alpha = \Delta H_f / \Delta H_{f100\%}$$

where  $\Delta H_f$  is melting enthalpy and  $\Delta H_{f100\%}$  is the difference between the enthalpy curves of completely amorphous LDPE and the pure crystalline material. The value of percentage crystallinity of LDPE was found to be 18.44%, which was reduced on addition of fly ash particles. A further addition of fly ash did not yield in lowering the crystallinity of LDPE. It appears that three phenomenon took place simultaneously: (1) engaging the amorphous part present in LDPE by fly ash, (2) locating themselves in interlamellar space of LDPE by the additional fly ash, and (3) providing nucleation sites to LDPE for the development of crystallites by fly ash. The initial reduction in crystalline might be an outcome of first two phenomenon as stated above; however the additional fly ash did not affect the overall crystallinity of LDPE due to a possible balancing of last two phenomenon. A little variation in crystallinity of LDPE

with the addition of fly ash was observed as shown in the Table II. The method used for determining crystallinity is based on values of enthalpy of corresponding sample. The sample size is very small, a few milligrams only for a DSC measurements. Attaining uniformity in milligram level for composites such as fly ash filled LDPE is a tough task and therefore minor variations in measuring enthalpy may affect the value of crystallinity. It can be summarized that the addition of fly ash particles resulted in small changes in the crystallinity of LDPE.

Figure 5 shows the variation in shear stress versus shear rate for different compositions of fly ash filled LDPE at 200°C. The shear stress increased with the shear rate in all cases. Similar plots were obtained at 160°C and 180°C for these materials but not shown here. The relationship between the shear rate ( $\dot{\gamma}$ ) and shear stress ( $\tau$ ) was as per Power law.

$$\tau = K\dot{\gamma}^n$$

where  $n$  is the index of pseudoplasticity and  $K$  is proportionality constant. The increase in shear stress was observed with loading of fly ash particles in the studied samples. The nature of all the curves is

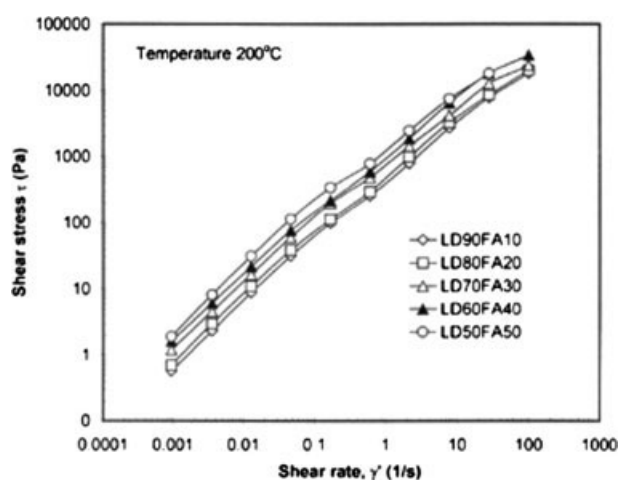
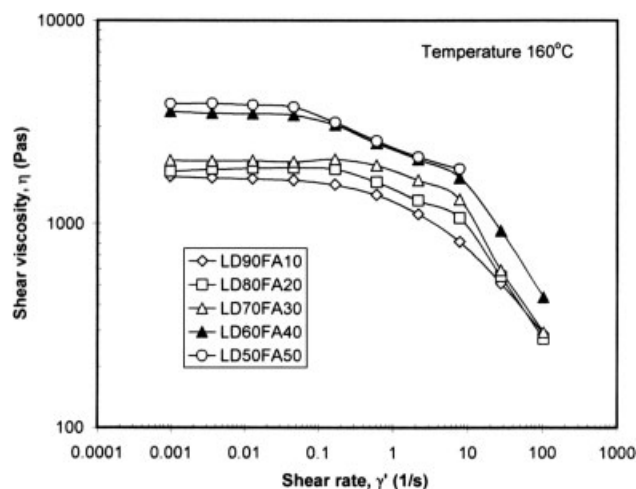


Figure 5 Plot between the shear stress and the shear rate at 200°C for different compositions of fly ash filled LDPE.



**Figure 6** Plot between viscosity and shear rate at 160°C for different compositions of fly ash filled LDPE.

similar. The values of  $n$  and  $K$  were determined using trend lines as per power law. The variation in  $n$  for different specimen was from 0.84 to 0.89, which can be considered as almost negligible with in the experimental errors for such a wide range of compositions and temperatures. The constant  $K$  showed significant increase with fly ash loading in LDPE; for example,  $K$  values for 0, 10, 20, 30, 40, and 50 wt % fly ash in LDPE at 160°C was found as 823, 923, 1038, 1180, 1739, and 2428 Pa s. The trend was similar at 180°C and 200°C. This observation implies that the increased shear stress with the increased loading of fly ash particles may be attributed to the restrictions offered by particles to the slippage of molecular chain of polymer during shear.

Figure 6 shows the changes in shear viscosity with shear rate at 160°C. For fly ash filled LDPE composites the shear viscosity shows two different trends in the entire range of shear rate. At low shear rates,

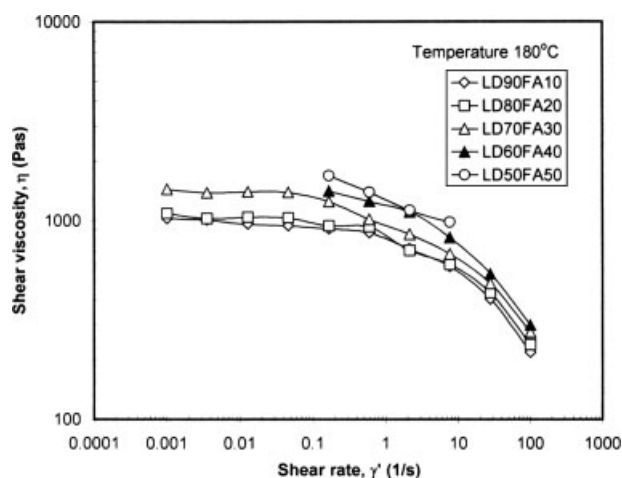


**Figure 7** Plot between viscosity and shear rate at 180°C for different compositions of fly ash filled LDPE.

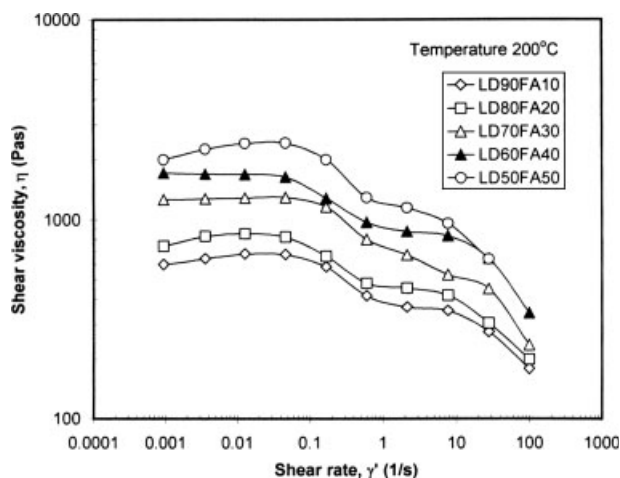


**Figure 8** Plot between viscosity and shear rate at 200°C for different compositions of fly ash filled LDPE.

the viscosity of system, irrespective of loading of fly ash particles in LDPE remained constant and behaved like Newtonian fluid; once the shear rate increased beyond  $0.01 \text{ s}^{-1}$ , the shear-thinning effect was observed. The increased viscosity with the increased content of fly ash may be attributed to the resistance offered by the filler particle. The shear thinning is attributed to the alignment of chains of polymer in the flow direction and thereby reducing viscosity of molten composite.

Figures 7 and 8 are similar plots showing the variations in the viscosity with the shear rate at temperatures 180°C and 200°C, respectively. Both these figures are similar in nature to Figure 5 but the corresponding values of viscosity of different compositions are comparatively less than those at 160°C. The increase in temperature reduced the viscosity of material. The shear thinning effect is more pronounced at 160°C as compared to that at 180°C or 200°C. Figure 8 is comparatively different than those of Figures 6 and 7. This figure shows two regions of shear thinning instead of single region for fly ash filled LDPE. At low shear-rate region a transition from Newtonian to non-Newtonian was observed; thereafter a second transition was also observed at higher shear rate region. A careful observation reveals that such behavior was more clearly observed in samples, which were having higher fractions of fly ash particles. It may be attributed to a temporary structure formed by the dispersed particles in-addition to the entangled polymeric chains. Now both the structures were sheared and offered resistance to flow. The characteristic shear thinning of LDPE was observed in high shear region whereas temporary network formed by the fly ash particles was observed at low shear rate. The region corresponding to particle network could not be detected at lower temperatures 160°C and 180°C because of the following

possibilities. The over all viscosity of system may be considered as the sum of the effects of (a) chain entanglement of polymer, (b) resistance offered to slippage of molecular chains by the particles entrapped between chains of polymer, and (c) particle-particle interaction/network. The factor (a) dominates the viscosity pattern at low temperatures and becomes less effective at the higher temperatures. On the other hand, the fly ash particles are sufficiently stable material at these temperatures as compared to the LDPE. Therefore this effect was observed at 200°C. The similar networks formed by the fine calcium carbonate particles and carbon black in the molten polymers were reported in literature.<sup>14,15</sup>

The polymeric fluid display normal stresses during shear flow that implies finite elastic strain developed in this fluid. These stresses have their origin in elasticity of liquids and are generally expressed in terms of principal stresses. The first normal stress difference  $N_1$  is approximately proportional to amount of shear. At low shear rates  $N_1$  is almost negligible as compared to tangential stresses but increases with increasing recoverable shear.<sup>16-18</sup> The shear rate dependence of  $N_1$  changes from first order for textured materials<sup>17</sup> to second ordered for homogeneous polymers<sup>18</sup> due to shear-induced homogenization at high shear region. In present case  $N_1$  is plotted against shear rate for different compositions of fly ash filled LDPE at two different temperatures as is shown in Figure 9. The values of  $N_1$  at 160°C are higher as compared to those at 200°C. The addition of fly ash particles reduced the values of  $N_1$  those were observed in each case. At low shear rates  $N_1$  is almost invariable with shear rate however it increases with shear rate once the shear rate is more than  $1.0 \text{ s}^{-1}$ . The values corresponding to 180°C fall in between the set of values corresponding to 160°C and 200°C but not displayed in this plot to maintain

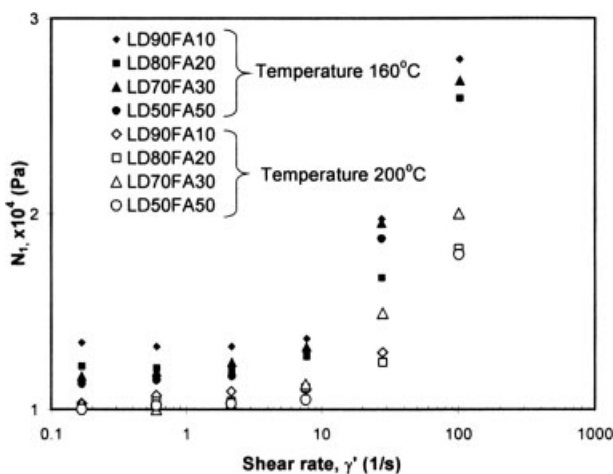


Figure 9 Variation in  $N_1$  with shear rate for different compositions of fly ash filled LDPE.

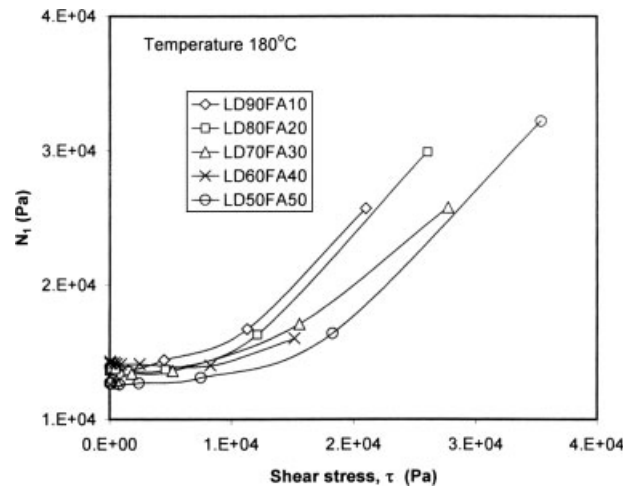


Figure 10 Plot between  $N_1$  and shear stress at 180°C for different compositions of fly ash filled LDPE.

clarity in the figure. Another plot between  $N_1$  and shear stress is shown in Figure 10. It displays that at low shear stresses the first normal stress difference does not vary significantly; however at higher shear stresses it increases with shear. It was also noticed that an addition of fly ash in LDPE decreased the value of  $N_1$ . This may be attributed to the reduced amount of recoverable strain in the system on addition of rigid fly ash particles. The recoverable shear strain,  $\gamma_R$  is an important parameter related to the elasticity of fluid and is estimated using following relationship

$$2\gamma_R\tau_w = N_1$$

The recoverable shear strain,  $\gamma_R$  increases with shear-rate and decreases with filler contents.<sup>19</sup> The replacement of polymeric material LDPE by rigid particles of fly ash reduces the recoverable elastic strain  $\gamma_R$ . This reduction in  $\gamma_R$  may be responsible for an overall reduction in  $N_1$  on addition of fly ash in LDPE as shown in Figures 9 and 10.

### CONCLUSIONS

The specimens containing different volume fractions of ultrafine fly ash in LDPE were prepared and examined for the thermal and rheological properties. The addition of ultrafine fly ash in LDPE decreased the melting enthalpy of the specimen. The crystallinity of LDPE decreased slightly with the addition of fly ash. The shear stress and shear viscosity both increased with the addition of ultrafine fly ash in LDPE. The first normal stress difference reduced with fly ash content and with the increased temperature. The values of  $N_1$  remained almost invariable at

low shear region however a proportional increase was observed beyond the shear stress of 10 kPa.

The authors are thankful to Dr. N. Ramakrishnan, Director, Advanced Materials and Processes Research Institute (AMPRI), Bhopal, for granting permission to publish this work. One of the authors (S.A.R.H.) is highly thankful to Dr. M. Saxena of AMPRI, Bhopal, for arranging fly ash and to Mr. T.S.V.C. Rao for helping in SEM study.

## References

1. Bare, W.; Albano, C.; Reyes, J.; Domínguez, N. *Surf Coat Technol* 2002, 158, 404.
2. Kuljanin, J.; Vučković, M.; Comor, M. I.; Bibić, N.; Djoković, V.; Nedeljković, J. M. *Eur Polym J* 2002, 38, 1659.
3. Weidenfeller, B.; Hofer, M.; Schilling, F. R. *Compos A: Appl Sci Manuf* 2004, 35, 423.
4. Yang, L.; Schruben, D. L. *Polym Eng Sci* 1994, 34, 1109.
5. Dang, Z.-M.; Zhang, Y.-H.; Tjong, S.-C. *Synth Metals* 2004, 146, 79.
6. Chand, N.; Jain, D. *J Appl Polym Sci* 2006, 100, 1269.
7. Hundiwale, D. G.; Kapadia, U. R.; Desai, M. C.; Patil, A. G.; Bidkar, S. H. *Polym Plast Technol Eng* 2004, 43, 615.
8. Bose, S.; Mahanwar, P. A. *J Appl Polym Sci* 2006, 99, 266.
9. Huang, X.; Wang, J. H.; Gills, J. M. *J Miner Mater Charact Eng* 2003, 2, 11.
10. Chand, N.; Vashishtha, S. R. *Bull Mater Sci* 2000, 23, 103.
11. [www.teriin.org/energy/fly\\_ash.htm](http://www.teriin.org/energy/fly_ash.htm).
12. Luyt, A. S.; Molefi, J. A.; Krump, H. *Polym Degrad Stabil* 2006, 91, 1629.
13. Schubnell, M. *User Com, Mettler Toledo-Thermal Analysis System* 2001, 1, 12.
14. Li, L.; Masuda, T. *J Soc Rheol Jpn* 1989, 17, 145.
15. Yano, S.; Kitano, T. In *Handbook of Applied Polymer Processing Technology*; Cherimisinoff, P. N., Ed.; Marcell Dekker: New York, 1996; p 125.
16. Hashmi, S. A. R.; Kitano, T. *Appl Rheol* 2006, 16, 152.
17. Onuki, A. *Phys Rev A* 1987, 35, 5149.
18. Ferry, J. D. *Viscoelastic Properties of Polymers*, 3rd ed.; Wiley: New York, 1980.
19. Chand, N.; Hashmi, S. A. R.; Vashishtha, S. R. *Ind J Eng Mater Sci* 1996, 3, 253.